Ultra-High Energy Cosmic Rays: A Probe of Physics and Astrophysics at Extreme Energies

Günter Sigl
Institut d'Astrophysique de Paris, 98bis Boulevard Arago, CNRS
75014 Paris, France

April 17, 2001

The origin of cosmic rays is one of the major unresolved questions in astrophysics. In particular, the highest energy cosmic rays observed possess macroscopic energies and their origin is likely associated with the most energetic processes in the Universe. They thus provide a probe of physics and astrophysics at energies that are unreached in laboratory experiments. Theoretical explanations range from acceleration of charged particles in astrophysical environments to particle physics beyond the well established Standard Model, and processes taking place at the earliest moments of our Universe. Distinguishing between these scenarios requires detectors with effective areas in the 1000 km^2 range which are now under construction or in the planning stage. Close connections with gamma-ray and neutrino astrophysics add to the interdisciplinary character of this field.

High energy cosmic ray (CR) particles are shielded by the Earth's atmosphere and reveal their existence on the ground only by indirect effects such as ionization and showers of secondary charged particles covering areas up to many km^2 for the highest energy particles. In fact, in 1912 Victor Hess discovered CRs by measuring ionization from a balloon [1], and in 1938 Pierre Auger proved the existence of "extensive air showers" (EAS) caused by primary particles with energies above $10^{15}\,\mathrm{eV}$ by simultaneously observing the arrival of secondary particles in ground detectors many meters apart [2].

After almost 90 years of CR research, their origin is still an open question, with a degree of uncertainty increasing with energy [3]: Only below 100 MeV kinetic energy, where the solar wind shields protons coming from outside the solar system, the Sun must give rise to the observed proton flux. Above that energy the CR spectrum exhibits surprisingly little structure and is well approximated by broken power laws $\propto E^{-\gamma}$ (see Fig. 1): At the energy $E \simeq 4 \times 10^{15}\,\mathrm{eV}$ called the "knee", the flux of particles per area, time, solid angle, and energy steepens from a power law index $\gamma \simeq 2.7$ to one of index $\simeq 3.0$. The bulk of the CRs up to at least that energy is believed to originate within our Galaxy. Above the so called "ankle" at $E \simeq 5 \times 10^{18}\,\mathrm{eV}$, the spectrum flattens again to a power law of index $\gamma \simeq 2.8$. This latter feature is often interpreted as a cross over from a steeper Galactic component, which above the ankle cannot be confined by the Galactic magnetic field, to a harder component of extragalactic origin. At the highest energies there is no apparent end to the CR spectrum, and over the last few years giant air showers from CR primaries with energies exceeding $10^{20}\,\mathrm{eV}$ [4, 5] (see Fig. 2) have been detected. This represents up to 50 Joules in what appears to be one elementary particle, about 10^8 times higher than energies achievable in man made accelerators! The nature and origin of CRs above the ankle, which we will call ultra-high energy cosmic rays (UHECRs), and especially the ones above $10^{20}\,\mathrm{eV}$ are mysterious [6, 7] and will be the main focus of this review.

The conventional "bottom-up" scenario assumes that all high energy charged particles are accelerated in astrophysical environments, typically in magnetized astrophysical shocks. A general estimate of the maximal energy that can be achieved is given by the requirement that the gyroradius $r_g \simeq E/(ZeB)$ of the particle of charge Ze and energy E in a magnetic field B is smaller than the size R of the accelerator, in numbers

$$r_g \simeq 100\, Z^{-1} \left(\frac{E}{10^{20}\,\mathrm{eV}}\right) \left(\frac{B}{\mu\mathrm{G}}\right)^{-1} \mathrm{kpc}; \quad E \lesssim 10^{18}\, Z \left(\frac{R}{\mathrm{kpc}}\right) \left(\frac{B}{\mu\mathrm{G}}\right) \mathrm{eV}\,. \qquad (1)$$

Here, B is measured in micro Gauss (μG) and R in kilo parsec ($1\,\mathrm{pc} = 3.09 \times 10^{18}\,\mathrm{cm}$). Eq. (1) is an optimistic estimate since it neglects the finite lifetime of the accelerator and energy losses due to interactions with the ambient environment such as synchrotron radiation in the magnetic field and production of secondary particles. Apart from the different scales, the factors involved are the same ones which limit the maximal energy in accelerator laboratories. The remnants associated with Galactic supernova explosions have sizes up to $R \sim$ pc with magnetic fields up to the milli Gauss range. According to Eq. (1) they should thus be able to accelerate CRs at least up to the knee, possibly up to the ankle. This and the fact that the power required to maintain the cosmic ray density in our Galaxy is comparable to the kinetic energy output rate of Galactic supernovae suggests that supernovae are the predominant sources of CRs in this energy range. At higher energies powerful extragalactic objects such as active galactic nuclei (AGN) are envisaged [3]. However, the existence of UHECRs at energies around 10^{20} eV and above, assuming them to be one of the known electromagnetically or strongly interacting particles, poses at least three theoretical problems:

Extragalactic Sources and the "GZK Cutoff"

Interactions with the omnipresent 2.7 Kelvin cosmic microwave background radiation (CMB), which is a thermal relic of the big bang, limit the attenuation length of the highest energy particles to less than about 50 megaparsecs (Mpc). For example, in the rest frame of a nucleon of energy $E \gtrsim E_{th}$ the CMB will appear as a background of $\gamma-$rays of sufficiently high energy to allow the production of pions. The threshold energy is given by

$$E_{th} = \frac{m_\pi(m_N + m_\pi/2)}{\varepsilon} \simeq 6.8 \times 10^{19} \left(\frac{\varepsilon}{10^{-3}\,\mathrm{eV}}\right)^{-1} \mathrm{eV}\,, \qquad (2)$$

where m_N and m_π are the nucleon and pion mass, respectively, and $\varepsilon \sim 10^{-3}\,$eV is a typical CMB photon energy. For $E \gtrsim E_{th}$ the nucleon will loose a significant part of its energy on a length scale of $l_\pi \simeq 1/(\sigma_\pi n_{\mathrm{CMB}}) \simeq 20\,$Mpc, where $n_{\mathrm{CMB}} \simeq 422\,\mathrm{cm}^{-3}$ is the number density of CMB photons, and the pion production cross section $\sigma_\pi \sim 100\,\mathrm{mbarn} = 10^{-25}\,\mathrm{cm}^2$. Nuclei and $\gamma-$rays have similar energy loss distances due to photodisintegration and electron-positron pair production on the CMB, respectively [6]. Therefore, if the CR sources were all at cosmological distances (i.e. several thousand Mpc away), the energy spectrum would exhibit a depletion of particles above a few $10^{19}\,$eV, the so-called Greisen-Zatsepin-Kuzmin (GZK)[8] cutoff. Since the data do not confirm such a cutoff [4, 5] (see Fig. 2), an astrophysical origin would require the sources to be within about 100 Mpc. The only way to avoid this conclusion without invoking as yet unknown new physics is that charged particles accelerated in sources at much larger distances give rise to a secondary neutrino beam which can propagate unattenuated. This neutrino beam has to be sufficiently strong to produce the observed UHECRs within 100 Mpc by electroweak (EW) interactions with the relic neutrino background, the neutrino analogue of the CMB [9]. However, this requires extremely powerful sources and local relic neutrino overdensities that hardly seem consistent with commonly accepted ideas about cosmic structure formation [10]. In addition, to avoid excessive fluxes at lower energies, the sources have to be nearly opaque to $\gamma-$rays and nucleons [10].

The Maximal Acceleration Energy Problem

Evaluating the maximum energy estimates in Eq. (1) for known astrophysical objects demonstrates that only very few such objects seem capable of accelerating charged particles up to a few 10^{20} eV [11]. In our Galactic neighbourhood, pulsars with magnetic fields larger than 10^{12} G satisfy the criterion Eq. (1) for iron nuclei. But it remains to be seen if energy losses in the dense pulsar environment do not considerably decrease the maximum energy [12]. Another interesting but highly speculative suggestion is the acceleration of particles to such energies in ultrarelativistic jets from bipolar supernovae in our Galaxy [13]. In general, Galactic sources tend to predict UHECR arrival directions correlated with Galactic structures, which is not seen in the data (see below). Possible extragalactic accelerators include AGN, radio galaxies [14], shock waves associated with large scale structure formation [15], and possibly $\gamma-$ray bursts. AGN are numerous enough, but are unlikely to reach the requisite energies, due to strong energy losses in the intense radiation fields of the cores. Hot spots in the jets of radio galaxies are sufficiently tenuous to avoid excessive energy losses, and extend up to kpc scales. With fields in the milli Gauss regime they meet the requirement Eq. (1) and synchrotron observations even seem to require the presence of protons up to $\sim 10^{21}$ eV in these objects [16]. The main problem is that such objects are rare [14]. Gamma-ray bursts, another as yet not understood enigma of astrophysics, have been observed to occur with a rate of about one burst within 100 Mpc (the maximal source distance for nucleons) per 100 years, each emitting up to $\sim 10^{54}$ ergs in $\gamma-$rays (depending on the unknown amount of beaming) within a few seconds. Therefore, if $\gamma-$ray bursts are to explain the few dozens of UHECRs observed within the past few decades above the GZK cutoff, they have to meet the following requirements: They must emit at least as much energy in the form of UHECRs as in $\gamma-$rays in the MeV range [17], the UHECRs must be charged, and their arrival times must be spread out by at least a few hundred years. The latter requires large scale magnetic fields stronger than about 10^{-10} G on Mpc scales [18].

Angular Distributions and Missing Counterparts

The seeming isotropy on large angular scales (with a possibly significant interesting clustering on degree scales) of arrival directions up to the highest energies [19] leaves only two possibilities for the source locations: Either there must be many nearby sources, at least one close to each arrival direction. Sufficiently powerful astrophysical accelerators which meet the above criteria are rare and should easily be detected within 100 Mpc, but no convincing source candidates have been found [20]. Or, alternatively, there are only very few nearby sources which then requires strong deflection in Galactic and/or extragalactic magnetic fields within a few Mpc propagation length. Eq. (1) shows that this requires fields of at least $\sim 10^{-7}$ G on Mpc scales. Such high field strengths are indeed expected to be localized in sheets and clusters of galaxies, but are hard to measure directly [21]. These values are also close to upper limits established from independent observations such as the frequency dependent Faraday rotation of the polarization of radio emission from distant sources in intervening magnetic fields [22].

Whether the expected distribution and strength of magnetic fields associated with large scale galaxy structure are consistent with UHECR spectra and angular distributions is currently under investigation [23]. As an example [24], Fig. 3 shows predictions for the distribution of arrival times and energies, the sky averaged spectrum, and the angular distribution of arrival directions in Galactic coordinates. In this scenario the UHECR sources are continuously distributed according to the matter density in the Local Supercluster, following an idealized pancake profile with scale height of 5 Mpc and scale length 20 Mpc, with no sources within 2 Mpc from the observer. All sources inject an $E^{-2.4}$ proton spectrum up to 10^{22} eV. The square of the magnetic field has a Kolmogorov spectrum with a maximal field strength $B_{\rm max} = 5 \times 10^{-7}$ G in the plane center, and also follows the matter density. The observer is within 2 Mpc of the Supergalactic Plane whose location is indicated by the solid line in the lower panel and at a distance $d = 20$ Mpc from the plane center. This example demonstrates the two major points of scenarios with large scale fields up to a micro Gauss: First, a steepening of the UHECR spectrum in the diffusive regime *below* $\sim 10^{20}$ eV may help to explain the observed spectrum at least down to 10^{19} eV with only one source component [25]. It is not clear, however, if the predicted flux is high enough above 10^{20} eV. Second, the predicted sky distribution may still not be isotropic enough unless the sources are not strongly correlated with the large scale galaxy structure.

Generally, magnetic fields down to $\sim 10^{-11}$ G can leave observable imprints on UHECR arrival time, energy and direction distributions [6, 26]. This may also help to make progress in the question of "magnetogenesis", the origin of galactic and cosmological magnetic fields, which likely have been seeded in the early Universe [27].

The enigma of UHECR origin is in a certain way opposite to the dark matter problem: Dark matter is expected to exist because of cosmological reasons [28] but has not been found yet, whereas UHECRs above the GZK cutoff were not expected to exist but are convincingly observed! In recent years this challenge triggered many theoretical proposals for the origin of these highest energy particles in the Universe, as well as new experimental projects and the study of new detection concepts. We first summarize the experimental activities.

Pioneering Experiments and New Detection Concepts

Above $\sim 10^{14}\,\mathrm{eV}$, the showers of secondary particles created by interactions of the primary CRs in the atmosphere are extensive enough to be detectable from the ground. In the most traditional technique, charged hadronic particles, as well as electrons and muons in these EAS are recorded by detecting the Cherenkov light that they emit when passing through water tanks, or by using scintillation counters. Apart from earlier experiments that were operative between the 1960s and 1980s [5], this technique is used by the largest operating ground array, the Akeno Giant Air Shower Array (AGASA) near Tokyo, Japan, covering an area of roughly $100\,\mathrm{km}^2$ with about 100 detectors of a few meters in size, mutually separated by about 1 km [29]. Given a flux of about one particle per km^2 per century above $10^{20}\,\mathrm{eV}$ (see Fig. 2), the detection rate for such particles is less than one per year with such an instrument. The ground array technique allows one to measure a lateral cross section of the shower profile and to estimate the energy of the shower-initiating primary particle from the density of secondary charged particles.

EAS can also be detected via the virtually isotropic fluorescence emission of the air nitrogen that they excite. A system of mirrors and photomultipliers in the form of an insect's eye can be used to track the longitudinal development of EAS. This technique was first used by the Fly's Eye detector [30] and will be part of several future projects on UHECR detection (see below). The primary energy can be estimated from the total fluorescence yield and the longitudinal shower shape contains information about the primary composition. Comparison of CR spectra measured with the ground array and the fluorescence technique indicate systematic errors in energy calibration that are generally smaller than $\sim 40\%$ [5].

An upscaled version of the old Fly's Eye experiment, the High Resolution Fly's Eye detector already takes data in Utah, USA [31]. Taking into account a duty cycle of about 10% (a fluorescence detector requires clear, moonless nights), this instrument will collect events above $10^{17}\,\mathrm{eV}$ at a rate about 10 times larger than for the old Fly's Eye. Another project utilizing the fluorescence technique is the Japanese Telescope Array [32] which is currently in the proposal stage. If approved, its collecting power will also be about 10 times that of the old Fly's Eye above 10^{17} eV. The largest project presently under construction is the Pierre Auger Giant Array Observatory [33] planned for two sites, one in Mendoza, Argentina and another in Utah, USA for maximal sky coverage. Each site will have a $3000\,\mathrm{km}^2$ ground array. The southern site will have about 1600 particle detectors (separated by 1.5 km each) overlooked by four fluorescence detectors. The ground arrays will have a duty cycle of nearly 100%, leading to detection rates about 30 times as large as for the AGASA array, i.e. about 50 events per year above 10^{20} eV. About 10% of the events will be detected by both the ground array and the fluorescence component and can be used for cross calibration and detailed EAS studies. The detection energy threshold will be around 10^{18} eV.

An old idea envisages to detect EAS in the Earth's atmosphere from space. This would provide an increase by another factor ~ 50 in collecting power compared to the Pierre Auger Project, i.e. an event rate above 10^{20} eV of up to a few thousand per year. Two concepts are currently being studied, the Orbiting Wide-angle Light-collector (OWL) [34] in the USA and the Extreme Universe Space Observatory (EUSO) [35] in Europe of which a prototype may fly on the International Space Station.

Space-based detectors would be especially suitable for detection of very small event rates such as those caused by neutrino primaries which rarely interact in the atmosphere due to their small interaction cross sections. This disadvantage for the detection process is at the same time a blessing since it makes these elusive particles reach us unattenuated over cosmological distances and from very dense environments where all other particles (except gravitational waves) would be absorbed. Giving rise to showers typically starting deep within the atmosphere, they are also easy to distinguish from other primaries. Besides detection from space, several other concepts are currently under study. These include detection of near-horizontal air showers with ground arrays [36], and detection of radio pulses emitted by neutrino induced electromagnetic showers within large effective volumes (see Ref. [6] for more details).

All these experimental concepts aim at probing existing theoretical concepts on the yet unknown origin of the highest-energy particles in the Universe or discovering new physics at energies unreachable in the laboratory. Let us now give an idea of what may be in store in terms of new physics.

Relics from the Early Universe

The apparent difficulties of bottom-up acceleration scenarios discussed earlier motivated the proposal of the "top-down" scenarios, where UHECRs, instead of being accelerated, are the decay products of certain sufficiently massive "X" particles produced by physical processes in the early Universe. Furthermore, particle accelerator experiments and the mathematical structure of the Standard Model of the weak, electromagnetic and strong interactions suggest that these forces should be unified at energies of about 2×10^{16} GeV (1 GeV= 10^9 eV) [37], 4-5 orders of magnitude above the highest energies observed in CRs. The relevant "Grand Unified Theories" (GUTs) predict the existence of X particles with mass m_X around this GUT scale. If their lifetime is comparable or larger than the age of the Universe, they would be dark matter candidates and their decays could contribute to UHECR fluxes today, with an anisotropy pattern that reflects the expected dark matter distribution. However, in many GUTs supermassive particles are expected to be very short lived and thus have to be produced continuously if their decays are to give rise to UHECRs. This can only occur by emission from topological defects which are relics of cosmological phase transitions that could have occurred in the early Universe at temperatures close to the GUT scale. Topological defects necessarily occur between regions that are causally disconnected, such that the orientation of the order parameter associated with the phase transition can not be communicated between these regions and thus will adopt different values. Examples are cosmic strings (similar to vortices in superfluid helium), magnetic monopoles, and domain walls (similar to Bloch walls separating regions of different magnetization in a ferromagnet). The defect density is consequently given by the particle horizon in the early Universe and their formation can by analogy even be studied in solid state experiments where the expansion rate of the Universe corresponds to the quenching speed that is applied to induce the transition [38]. The defects are topologically stable, but in the case of GUTs time dependent motion can lead to the emission of GUT scale X particles.

It is interesting to note that one of the prime cosmological motivations to postulate inflation, a phase of exponential expansion in the early Universe [28], was to dilute excessive production of "dangerous relics" such as topological defects and superheavy stable particles. However, right after inflation, when the Universe reheats, phase transitions can occur and such relics can be produced in cosmologically interesting abundances, and with a mass scale roughly given by the inflationary scale. This scale is fixed by the CMB anisotropies to $\sim 10^{13}$ GeV [39]. The reader will notice that this mass scale is not far above the highest energies observed in CRs, thus motivating a connection between these primordial relics and UHECRs which in turn may provide a probe of the early Universe!

Within GUTs the X particles typically decay into jets of particles whose spectra can be well estimated within the Standard Model. Before reaching Earth, the injected spectra are reprocessed by interactions with the low energy photon backgrounds such as the CMB, and magnetic fields present in the Universe (see Ref. [6, 42] for details). Fig. 4 shows a typical example for the UHECR spectrum expected in top-down scenarios: The observed flux is reproduced above 3×10^{19} eV; at lower energies where the Universe is transparent to nucleons, bottom-up mechanisms could explain the spectrum without significant problems. The X particle sources are not necessarily expected to be associated with astrophysical objects, but their distribution has to be sufficiently continuous to be consistent with observed angular distributions.

The most characteristic features are visible in Fig. 4: Electromagnetic cascades induced by interactions of the injected particles with the low energy photon backgrounds lead to a strong contribution to the diffuse $\gamma-$ray flux between 30 MeV and 100 GeV, close to the flux measured by the EGRET detector flown on board the Compton $\gamma-$ray Observatory satellite [40]. The energy content in these $\gamma-$rays is comparable to the one in the ultra-high energy neutrino flux which should be detectable with next generation experiments (see Fig. 4). The neutrino flux is hardly influenced by subsequent interactions, and thus directly represents the decay spectrum. In bottom-up scenarios neutrinos can only be produced as secondaries and for sources transparent to the primary nucleons the neutrino flux must be considerably smaller [43]. This can also serve as a discriminator between the top-down and bottom-up concepts. Finally, top-down models predict a significant $\gamma-$ray component above $\sim 10^{20}\,$eV, whereas nucleons would dominate at lower energies. This will be a strong discriminator as experiments will improve constraints on UHECR composition which currently seem to favor nucleons [44].

Besides some uncertainties in the shape and chemical composition of the spectrum, possibly the most significant shortcoming of top-down scenarios is their lack of predictivity concerning the absolute flux normalization. At least, the moderate rate of 10 decays per year in a spherical volume with radius equal the Earth-Sun distance, the rate necessary to explain the UHECR flux, is not in a remote corner of parameter space for most scenarios: Dimensional and scaling arguments imply that topological defects release X particles with an average rate at cosmic time t of

$$\dot{n}_X(t) = \kappa\, m_X^p\, t^{-4+p}\,, \qquad (3)$$

where the dimensionless parameters κ and p depend on the specific top-down scenario [6]. For example, hybrid defects involving cosmic strings have $p = 1$ and normalization of predicted spectra both at EGRET energies and around $10^{20}\,$eV, as shown in Fig. 4, leads to $\kappa m_X \sim 10^{13} - 10^{14}\,$GeV. For $\kappa \sim 1$, the resulting mass scale is again close to the inflation and GUT scales!

New Primary Particles and New Interactions

A possible way around the problem of missing counterparts in the framework of acceleration scenarios is to propose primary particles whose range is not limited by interactions with the CMB. The only established candidate is the neutrino. More speculatively, one could propose as yet undiscovered neutral particles which, according to Eq. (2), would have a higher GZK threshold if they are more massive than nucleons. In fact, in supersymmetric extensions of the Standard Model, new neutral hadronic bound states of light gluinos with quarks and gluons, so-called R-hadrons with masses in the 10 GeV range, have been suggested [45]. However, this possibility seems difficult to reconcile with accelerator constraints [46]. Magnetic monopoles and their bound states [47] as well as superconducting string loops [48] similarly have the advantage of not being degraded significantly by interactions with the CMB and can be efficiently accelerated. The main problematic issues with these primaries are the spectra, the atmospheric shower profiles, and (for non-relativistic monopoles) the arrival direction distributions. For example, the latter should show correlations with Galactic structures which are not observed. We will therefore here mostly focus on neutrinos.

To rescue the bottom-up scenario, the particle propagating over extragalactic distances, be it a neutrino or a new massive neutral hadron has to be produced in interactions of a charged primary which is accelerated in a powerful astrophysical object. In comparison to EAS induced by nucleons, nuclei, or $\gamma-$rays, the accelerator can now be located at cosmological distances. The cost of this conceptual advantage is an increase of the necessary charged primary energy to $\gtrsim 10^{22}\,\mathrm{eV}$ due to losses caused by the expansion of the Universe (redshift) and in the production of the secondary. These scenarios predict a correlation between UHECR arrival directions and sources at cosmological distances. Possible evidence for an angular correlation of events above the GZK cutoff with compact radio quasars at several thousand Mpc distance is currently being debated [49]. Only a few more events could settle the question!

Neutrino primaries have the advantage of being established particles. Unfortunately, within the Standard Model their interaction cross section with nucleons, $\sigma_{\nu N}$, falls short of producing ordinary air showers by about five orders of magnitude, with significant ramifications for their detection, as mentioned above. However, at (squared) center of mass (CM) energies s above the EW scale, corresponding to $\simeq 10^{15}\,\mathrm{eV}$ in the nucleon rest frame, this cross section has not been measured. Field theory constraints on the growth at higher energies based on unitarity are relatively weak [50]. Neutrino induced air showers above $10^{15}\,\mathrm{eV}$ may therefore rather directly probe new physics beyond the EW scale, if it leads to enhanced cross sections.

One theoretical possibility consists of a large increase in the number of degrees of freedom above the EW scale [51]. A specific implementation of this idea is provided by scenarios with additional large compact dimensions and a string or quantum gravity scale $M_s \sim \mathrm{TeV}$ ($= 10^{12}\,\mathrm{eV}$). This concept has recently received much attention in the literature [52] because it may imply unification of all forces in the TeV range, not far above the scale of EW interactions. This scenario would avoid the "hierarchy problem" between the EW scale $\simeq$ 100 GeV and the Planck scale $\simeq 10^{19}$ GeV of gravity. The cross sections within such scenarios have not been calculated from first principles yet, but several arguments based on unitarity lead to estimates that can very roughly be parametrized by [53]

$$\sigma_{\rm new} \simeq \frac{4\pi s}{M_s^4} \simeq 10^{-27} \left(\frac{M_s}{\rm TeV}\right)^{-4} \left(\frac{E}{10^{20}\,{\rm eV}}\right) {\rm cm}^2\,. \tag{4}$$

In the last expression we specified to a neutrino of energy E hitting a nucleon at rest. A neutrino would typically start to interact in the atmosphere for $\sigma_{\nu N} \gtrsim 10^{-27}\,{\rm cm}^2$, i.e. in the case of Eq. (4) for $E \gtrsim 10^{20}$ eV, assuming $M_s \simeq 1$ TeV, a value consistent with lower limits from accelerator experiments [54] and astrophysical constraints [55]. The neutrino therefore becomes a primary candidate for the observed UHECR events. Cross sections of the form Eq. (4) would predict the average atmospheric column depth of the first interaction point of neutrino induced EAS to depend linearly on energy. This signature should easily be distinguishable from the logarithmic scaling expected for nucleons, nuclei, and $\gamma-$rays.

Independent of theoretical arguments, the UHECR data can be used to put constraints on neutrino cross sections at energies not accessible in the laboratory: The Fly's Eye experiment has not seen any air showers developing deep in the atmosphere and has put a limit on their rate [59] (see Fig. 4). The existence of a secondary neutrino flux from the decay of pions produced in UHECR interactions with the CMB (marked "$N\gamma$ in Fig. 4) then implies that $\sigma_{\nu N}$ cannot be larger than the Standard Model cross section by more than a factor $\sim 10^3$ between 10^{18} eV and 10^{20} eV [56]. This conclusion can only be avoided if UHECRs do not have an extragalactic origin or if $\sigma_{\nu N}$ is comparable to hadronic cross sections, giving rise to normal EAS. The projected sensitivity of future experiments such as the Pierre Auger Observatories and the space based satellite projects (see Fig. 4) indicate that these cross section limits could be improved by up to four orders of magnitude.

Probably the most radical proposition concerns a violation of one of the basic symmetry principles of modern field theory such as Lorentz invariance. Such violations can kinematically prevent energy loss processes such as pion production at high Lorentz factors [57]. A reliable experimental determination of source distances and primary composition could confirm such symmetry violations or constrain them possibly more strongly than accelerator experiments [58].

Conclusions

UHECRs attest to perhaps the most energetic processes in the Universe. They are not only messengers of astrophysics at extreme energies, but may also open a window to particle physics beyond the Standard Model as well as probing processes occurring in the early Universe at energies close to the GUT scale. Furthermore, complementary to other methods such as Faraday rotation measurements, UHECRs can be used to probe the poorly known large scale cosmic magnetic fields and their origin. There seems to be no single convincing theoretical model for the UHECR origin yet and thus the solution to this problem will strongly depend on detailed measurements of energy distributions, arrival directions and times, and composition. The scientific community eagerly awaits the arrival of several large scale experiments under construction or in the proposal stage.

References

[1] V. F. Hess, *Phys. Z.* **13**, 1084 (1912).

[2] P. Auger, R. Maze, T. Grivet-Meyer, *Académie des Sciences* **206**, 1721 (1938); P. Auger, R. Maze, *ibid.* **207**, 228 (1938).

[3] for a general introduction on cosmic rays see, e.g., V. S. Berezinsky, S. V. Bulanov, V. A. Dogiel, V. L. Ginzburg, V. S. Ptuskin, *Astrophysics of Cosmic Rays* (North-Holland, Amsterdam, 1990); T. K. Gaisser, *Cosmic Rays and Particle Physics*, Cambridge University Press (Cambridge, 1998).

[4] M. Nagano, A. A. Watson, *Rev. Mod. Phys.* **72**, 689 (2000), and references therein.

[5] for a summary of the data situation and experimental issues see, e.g., S. Yoshida, H. Dai, *J. Phys. G* **24**, 905 (1998); X. Bertou, M. Boratav, A. Letessier-Selvon, *Int. J. Mod. Phys.* **A15**, 2181 (2000), and references therein.

[6] see, e.g., P. Bhattacharjee, G. Sigl, *Phys. Rep.* **327**, 109 (2000), and references therein.

[7] see, e.g., J. W. Cronin, *Rev. Mod. Phys.* **71**, S165 (1999); A. V. Olinto, *Phys. Rept.* **333-334**, 329 (2000); X. Bertou, M. Boratav, A. Letessier-Selvon, *Int. J. Mod. Phys.* **A15**, 2181 (2000).

[8] K. Greisen, *Phys. Rev. Lett.* **16**, 748 (1966); G. T. Zatsepin, V. A. Kuzmin, *Pis'ma Zh. Eksp. Teor. Fiz.* **4**, 114 (1966) [*JETP. Lett.* **4**, 78 (1966)].

[9] T. J. Weiler, *Phys. Rev. Lett.* **49**, 234 (1982); *Astrophys. J.* **285**, 495 (1984); *Astropart. Phys.* **11**, 317 (1999).

[10] S. Yoshida, G. Sigl, S. Lee, *Phys. Rev. Lett.* **81**, 5505 (1998); J. J. Blanco-Pillado, R. A. Vázquez, E. Zas, *Phys. Rev. D* **61**, 123003 (2000).

[11] A. M. Hillas, *Ann. Rev. Astron. Astrophys.* **22**, 425 (1984); C. A. Norman, D. B. Melrose, A. Achterberg, *Astrophys. J.* **454**, 60 (1995).

[12] P. Blasi, R. I. Epstein, A. V. Olinto, *Astrophys. J. Lett.* **533**, L123 (2000).

[13] A. Dar, R. Plaga, *Astron. Astrophys.* **349**, 259 (1999).

[14] see, e.g., P. L. Biermann, *J. Phys. G: Nucl. Part. Phys.* **23**, 1 (1997).

[15] H. Kang, J. P. Rachen, and P. L. Biermann, *Mon. Not. R. Soc. Astron.* **286**, 257 (1997).

[16] P. L. Biermann, P. A. Strittmatter, *Astrophys. J.* **322**, 643 (1987).

[17] F. Stecker, *Astropart. Phys.* **14**, 207 (2000).

[18] E. Waxman, *Phys. Scripta* **T85**, 117 (2000), and references therein.

[19] N. Hayashida et al., *Phys. Rev. Lett.* **77**, 1000 (1996); M. Takeda et al., *Astrophys. J.* **522**, 225 (1999); N. Hayashida *et al.*, e-print astro-ph/0008102.

[20] G. Sigl, D. N. Schramm, P. Bhattacharjee, *Astropart. Phys.* **2**, 401 (1994); J. W. Elbert, P. Sommers, *Astrophys. J.* **441**, 151 (1995).

[21] K. T. Kim et al., *Nature* **341**, 720 (1989); T. Clark, P. P. Kronberg, H. Böhringer, submitted to *Astrophys. J. Lett.*

[22] J. P. Vallee, *Fund. Cosm. Phys.* **19**, 1 (1997); P. Blasi, S. Burles, A. V. Olinto, *Astrophys. J.* **514**, L79 (1999).

[23] G. Medina Tanco, *Astrophys. J. Lett.* **505**, L79 (1998); T. Ensslin, e-print astro-ph/9906212; E.-J. Ahn, G. Medina-Tanco, P. L. Biermann, T. Stanev, e-print astro-ph/9911123; G. R. Farrar, T. Piran, *Phys. Rev. Lett.* **84**, 3257 (2000); T. Stanev, R. Engel, A. Muecke, R. J. Protheroe, J. P. Rachen, *Phys. Rev. D* **62**, 093005 (2000).

[24] M. Lemoine, G. Sigl, P. Biermann, e-print astro-ph/9903124.

[25] G. Sigl, M. Lemoine, P. Biermann, *Astropart. Phys.* **10**, 141 (1999); P. Blasi, A. V. Olinto, *Phys. Rev. D.* **59**, 023001 (1999).

[26] G. Sigl, M. Lemoine, *Astropart. Phys.* **9**, 65 (1998).

[27] see, e.g., D. Grasso, H. R. Rubinstein, e-print astro-ph/0009061, to appear in *Phys. Rept.*

[28] see, e.g., E. W. Kolb, M. S. Turner, *The Early Universe* (Addison-Wesley, Redwood City, California, 1990).

[29] N. Hayashida et al., *Phys. Rev. Lett.* **73**, 3491 (1994); S. Yoshida et al., *Astropart. Phys.* **3**, 105 (1995); M. Takeda *et al.*, *Phys. Rev. Lett.* **81**, 1163 (1998); see also http://icrsun.icrr.u-tokyo.ac.jp/as/project/agasa.html.

[30] D. J. Bird et al., *Phys. Rev. Lett.* **71**, 3401 (1993); *Astrophys. J.* **424**, 491 (1994); *ibid.* **441**, 144 (1995).

[31] S. C. Corbató *et al.*, *Nucl. Phys. B (Proc. Suppl.)* **28B**, 36 (1992); see also http://hires.physics.utah.edu/.

[32] M. Teshima et al., *Nucl. Phys. B (Proc. Suppl.)* **28B**, 169 (1992); see also http://www-ta.icrr.u-tokyo.ac.jp/.

[33] J. W. Cronin, *Nucl. Phys. B (Proc. Suppl.)* **28B**, 213 (1992); The Pierre Auger Observatory Design Report (2nd edition), March 1997; see also http://http://www.auger.org/ and http://www-lpnhep.in2p3.fr/auger/welcome.html.

[34] D. B. Cline, F. W. Stecker, OWL/AirWatch science white paper, e-print astro-ph/0003459; see also http://lheawww.gsfc.nasa.gov/docs/gamcosray/hecr/OWL/.

[35] See http://www.ifcai.pa.cnr.it/Ifcai/euso.html.

[36] J. J. Blanco-Pillado, R. A. Vázquez, E. Zas, *Phys. Rev. Lett.* **78**, 3614 (1997); K. S. Capelle, J. W. Cronin, G. Parente, E. Zas, *Astropart. Phys.* **8**, 321 (1998); A. Letessier-Selvon, e-print astro-ph/0009444.

[37] see, e.g., S. Weinberg, *The Quantum Theory of Fields Vol 2: Modern Applications*, Cambridge University Press (Cambridge, 1996).

[38] see, e.g., T. Vachaspati, *Contemp. Phys.* **39**, 225 (1998).

[39] for a brief review see V. Kuzmin, I. Tkachev, *Phys. Rept.* **320**, 199 (1999).

[40] P. Sreekumar *et al.*, *Astrophys. J.* **494**, 523 (1998).

[41] See, e.g., M. A. Lawrence, R. J. O. Reid, A. A. Watson, *J. Phys. G Nucl. Part. Phys.* **17**, 733 (1991), and references therein; see also http://ast.leeds.ac.uk/haverah/hav-home.html.

[42] G. Sigl, S. Lee, P. Bhattacharjee, S. Yoshida, *Phys. Rev. D* **59**, 043504 (1999).

[43] E. Waxman, J. Bahcall, *Phys. Rev. D.* **59**, 023002 (1999); J. Bahcall, E. Waxman, e-print hep-ph/9902383; K. Mannheim, R. J. Protheroe, J. P. Rachen, e-print astro-ph/9812398, to appear in *Phys. Rev. D.*; J. P. Rachen, R. J. Protheroe, K. Mannheim, e-print astro-ph/9908031.

[44] F. Halzen, R. A. V'azques, T. Stanev, H. P. Vankov, *Astropart. Phys.* **3**, 151 (1995); M. Ave, J. A. Hinton, R. A. V'azques, A. A. Watson, E. Zas, *Phys. Rev. Lett.* **85** 2244 (2000).

[45] G. R. Farrar, *Phys. Rev. Lett.* **76**, 4111 (1996); D. J. H. Chung, G. R. Farrar, E. W. Kolb, *Phys. Rev. D* **57**, 4696 (1998).

[46] I. F. Albuquerque *et al.* (E761 collaboration), *Phys. Rev. Lett.* **78**, 3252 (1997); A. Alavi-Harati *et al.* (KTeV collaboration), *Phys. Rev. Lett.* **83**, 2128 (1999).

[47] see S. D. Wick, T. W. Kephart, T. J. Weiler, P. L. Biermann, e-print astro-ph/0001233, and references therein.

[48] S. Bonazzola, P. Peter, *Astropart. Phys.* **7**, 161 (1997).

[49] G. R. Farrar, P. L. Biermann, *Phys. Rev. Lett.* **81**, 3579 (1998); C. M. Hoffman, *ibid.* **83**, 2471 (1999); G. R. Farrar, P. L. Biermann, *ibid.* **83**, 2472 (1999); G. Sigl, D. F. Torres, L. A. Anchordoqui, G. E. Romero, e-print astro-ph/0008363; A. Virmani *et al.*, e-print astro-ph/0010235.

[50] H. Goldberg and T. J. Weiler, *Phys. Rev. D* **59**, 113005 (1999).

[51] G. Domokos, S. Kovesi-Domokos, *Phys. Rev. Lett.* **82**, 1366 (1999).

[52] see, e.g., N. Arkani-Hamed, S. Dimopoulos, G. Dvali, *Phys. Rev. D* **59**, 086004 (1999).

[53] S. Nussinov, R. Shrock, *Phys. Rev. D* **59**, 105002 (1999); P. Jain, D. W. McKay, S. Panda, J. P. Ralston, *Phys. Lett.* **B484**, 267 (2000); J. P. Ralston, P. Jain, D. W. McKay, S. Panda, e-print hep-ph/0008153.

[54] see, e.g., S. Cullen, M. Perelstein, M. E. Peskin, *Phys. Rev.D* **62**, 055012 (2000), and references therein.

[55] S. Cullen, M. Perelstein, *Phys. Rev. Lett.* **83**, 268 (1999); V. Barger, T. Han, C. Kao, R.-J. Zhang, *Phys. Lett. B* **461**, 34 (1999).

[56] C. Tyler, A. Olinto, G. Sigl, e-print hep-ph/0002257.

[57] see, e.g., S. Coleman, S. L. Glashow, *Nucl. Phys.* **B574**, 130 (2000); L. Gonzalez-Mestres, *Nucl. Phys. B (Proc. Suppl.)* **48**, 131 (1996), and references therein.

[58] see, e.g., R. Aloisio, P. Blasi, P. L. Ghia, A. F. Grillo, *Phys. Rev. D* **62**, 053010 (2000).

[59] R. M. Baltrusaitis *et al.*, *Astrophys. J.* **281**, L9 (1984); *Phys. Rev. D* **31**, 2192 (1985).

[60] R. J. Protheroe, P. A. Johnson, *Astropart. Phys.* **4**, 253 (1996), and erratum *ibid.* **5**, 215 (1996).

[61] I acknowledge P. Biermann, P. Blasi, M. Boratav, T. Ensslin, P. Peter, R. Plaga, and G. Raffelt for very helpful comments on the manuscript.

Figure Captions

Fig. 1: The CR all-particle spectrum observed by different experiments above 10^{11} eV (from Ref [4] with permission). The differential flux in units of events per area, time, energy, and solid angle was multiplied with E^3 to project out the steeply falling character. The "knee" can be seen at $E \simeq 4 \times 10^{15}$ eV, and the "ankle" at $E \simeq 5 \times 10^{18}$ eV.

Fig. 2: Same as Fig. 1, but focusing on the high energy end above 10^{17} eV (from Ref [4] with permission). The "ankle" is again visible at $E \simeq 5 \times 10^{18}$ eV.

Fig. 3: The UHECR distribution of arrival times and energies (top), the sky averaged spectrum (middle, with 1 sigma error bars showing combined data from the Haverah Park [41], the Fly's Eye [30], and the AGASA [29] experiments above 10^{19} eV), and the sky distribution in Galactic coordinates (bottom, with color scale showing the intensity per solid angle) in the bottom-up scenario with sources in the local Supercluster of galaxies explained in the text. 20000 proton trajectories for 4 magnetic field realizations each were calculated. The cross-over from the diffusive regime below $\simeq 2 \times 10^{20}$ eV to the regime of rectilinear propagation at the highest energies is clearly visible in the two upper panels.

Fig. 4: All particle spectra for a top-down model involving the decay into two quarks of non-relativistic X particles of mass 10^{16} GeV, released from homogeneously distributed topological defects. Lower panel: The fluxes of the "visible" particles, nucleons and $\gamma-$rays. 1 sigma error bars are as in Fig. 3 (see also Fig. 2). Also shown are piecewise power law fits to the observed charged CR flux below 10^{19} eV, the measurement of the diffuse γ-ray flux between 30 MeV and 100 GeV by the EGRET instrument [40], as well as upper limits on the diffuse $\gamma-$ray flux from various experiments at higher energies (see Ref. [6] for more details). Upper panel: Neutrino fluxes. Shown are experimental neutrino flux limits from the Fly's Eye [59] and other experiments as indicated (see Ref. [6] for details), as well as projected neutrino sensitivities of the Pierre Auger Project [36] (for electron and tau neutrinos separately) and the proposed space based OWL [34] concept. For comparison also shown are the atmospheric neutrino background (hatched region marked "atmospheric"), and neutrino flux predictions for a model of AGN optically thick to nucleons ("AGN"), and for UHECR interactions with the CMB [60] ("$N\gamma$", dashed range indicating typical uncertainties for moderate source evolution). The top-down fluxes are shown for electron-, muon, and tau-neutrinos separately, assuming no (lower ν_τ-curve) and maximal $\nu_\mu - \nu_\tau$ mixing (upper ν_τ-curve, which would then equal the ν_μ-flux), respectively.

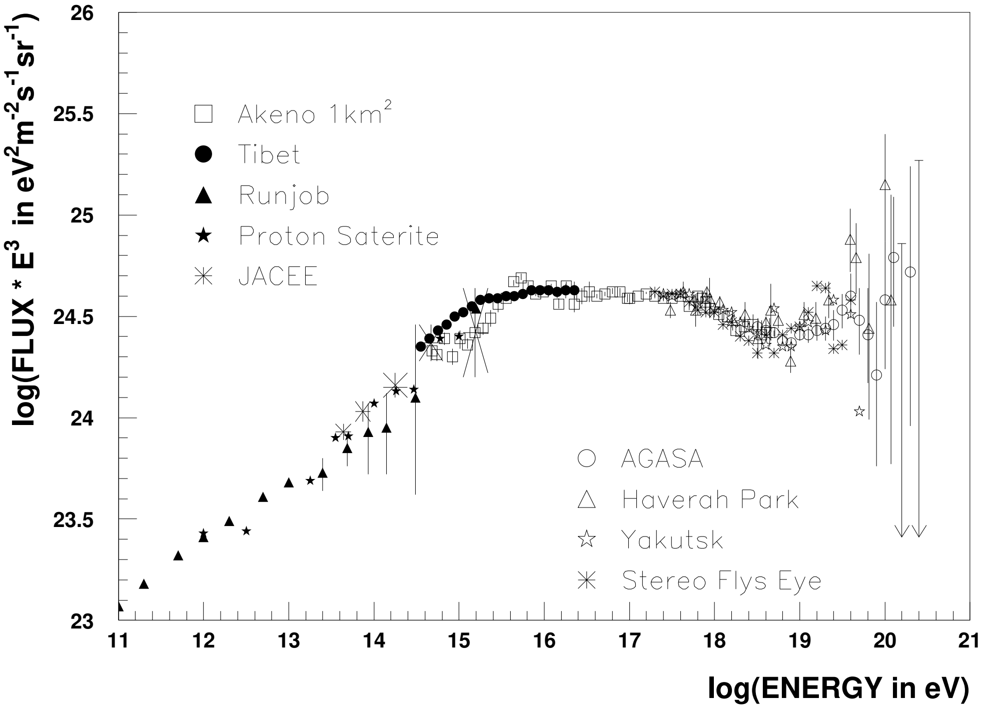

log(FLUX * E^3 in eV^{2}m^{-2}s^{-1}sr^{-1})
26
25.5
25
24.5
24
23.5
23
Akeno 1km^2
Tibet
Runjob
Proton Saterite
JACEE
AGASA
Haverah Park
Yakutsk
Stereo Flys Eye
11
12
13
14
15
16
17
18
19
20
21
log(ENERGY in eV)

Figure 1:

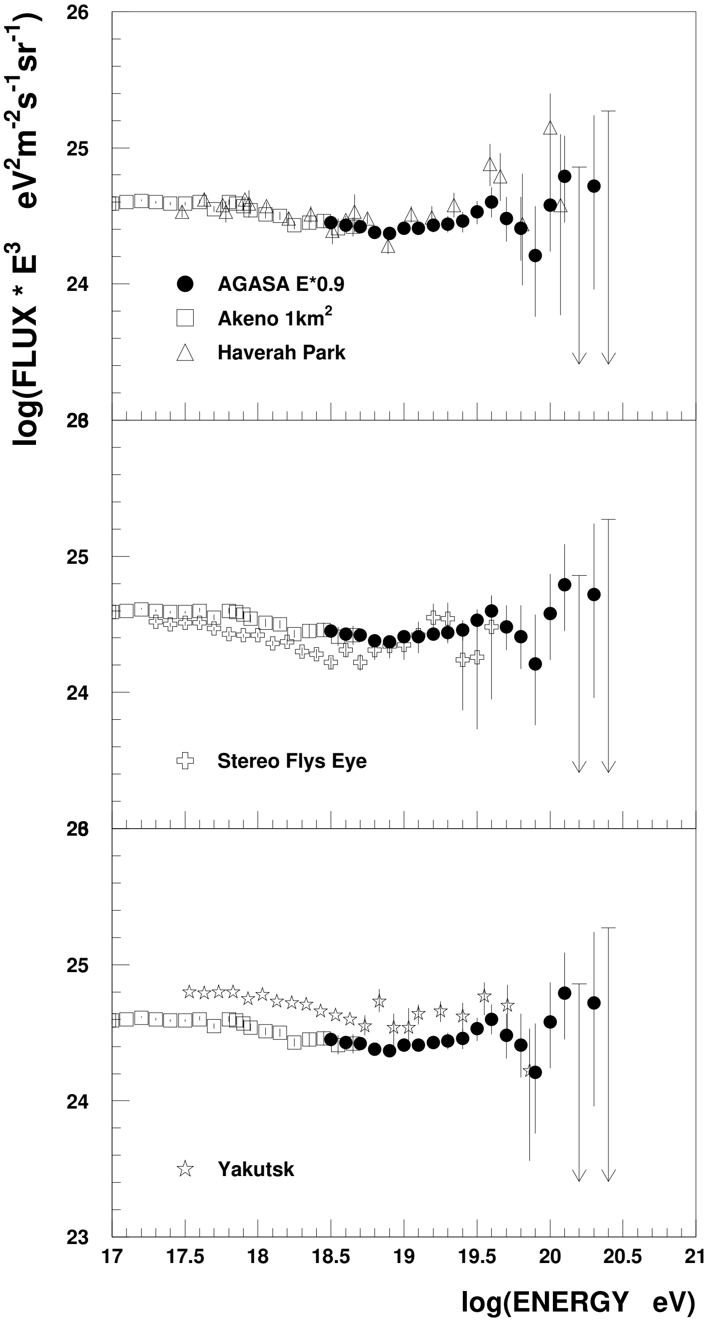

log(FLUX * E3 eV2m-2s-1sr-1)
26
25
24
28
25
24
28
25
24
23
AGASA E*0.9
Akeno 1km2
Haverah Park
Stereo Flys Eye
Yakutsk
17
17.5
18
18.5
19
19.5
20
20.5
21
log(ENERGY eV)

Figure 2:

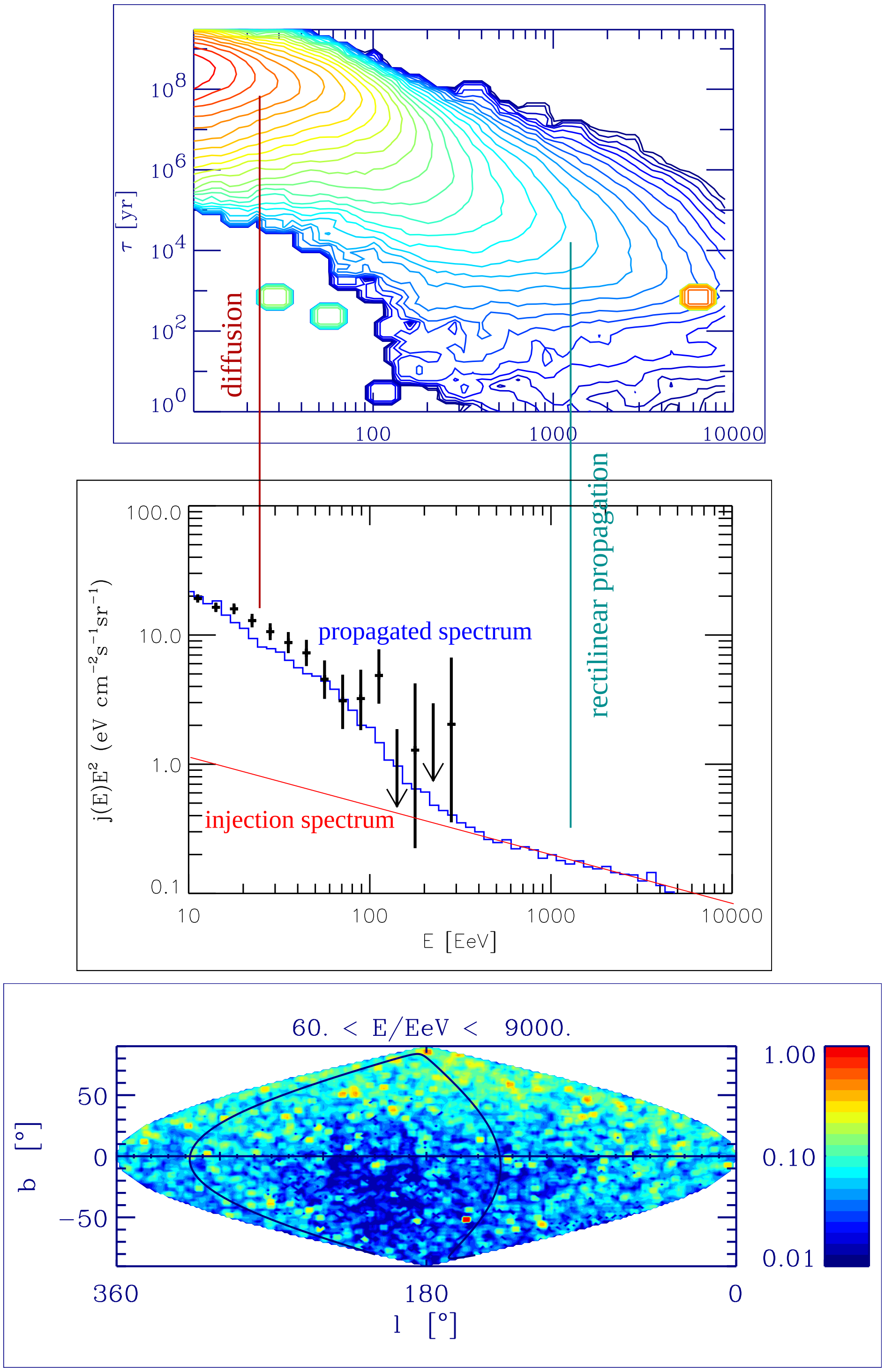

τ [yr]
diffusion
rectilinear propagation
j(E)E² (eV cm⁻²s⁻¹sr⁻¹)
propagated spectrum
injection spectrum
E [EeV]
60. < E/EeV < 9000.
b [°]
l [°]

Figure 3:

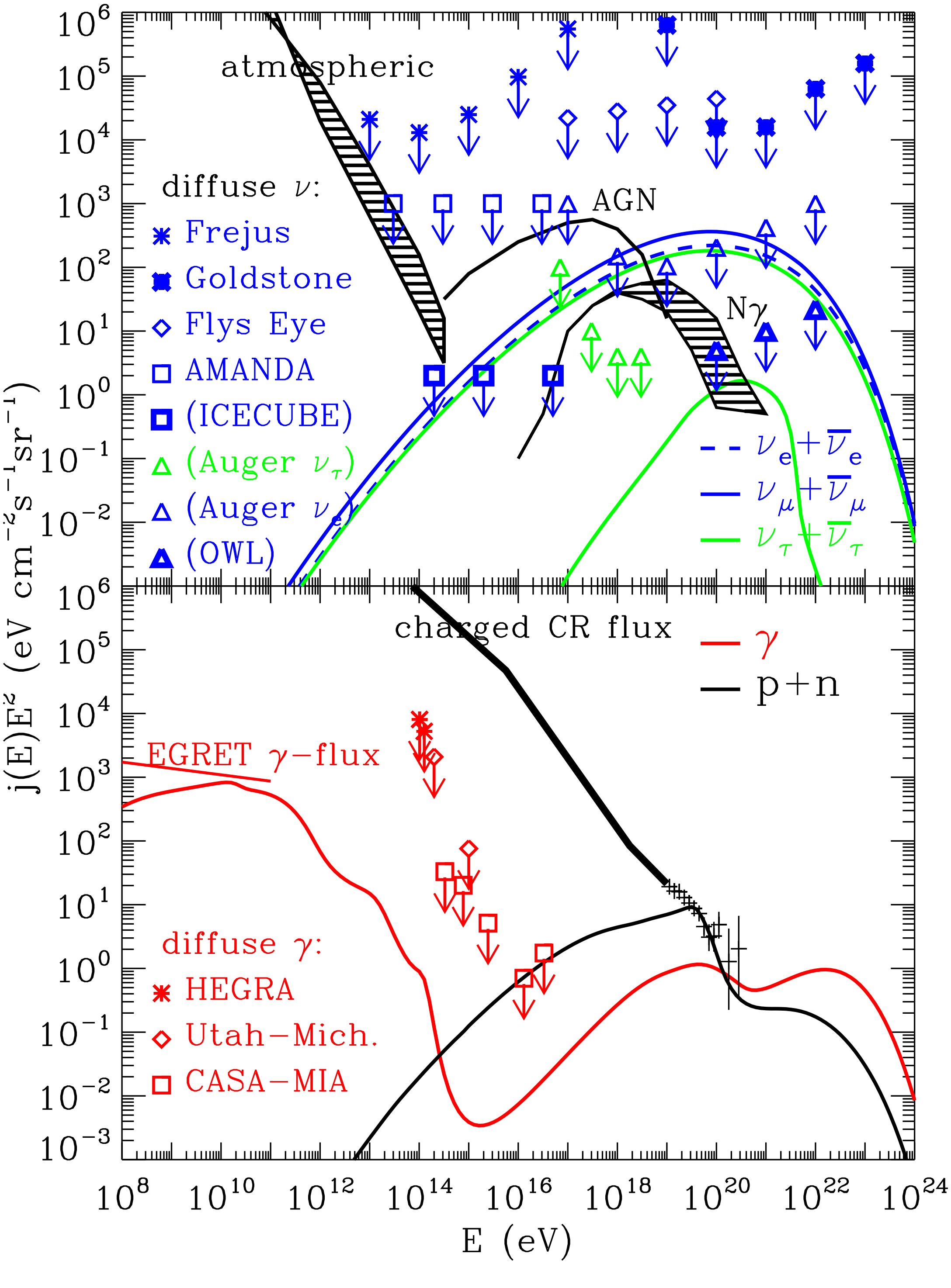

atmospheric
diffuse ν:
Frejus
Goldstone
Flys Eye
AMANDA
(ICECUBE)
(Auger ν_τ)
(Auger ν_e)
(OWL)
AGN
Nγ
ν_e + ν̄_e
ν_μ + ν̄_μ
ν_τ + ν̄_τ
charged CR flux
γ
p+n
EGRET γ−flux
diffuse γ:
HEGRA
Utah−Mich.
CASA−MIA
j(E)E² (eV cm⁻² s⁻¹ sr⁻¹)
E (eV)

Figure 4: